Electrical Power and Energy Systems 44 (2013) 656–665

Contents lists available at SciVerse ScienceDirect

Electrical Power and Energy Systems

journal homepage: www.elsevier.com/locate/ijepes

Robust voltage controller design for an isolated Microgrid using Kharitonov's theorem and D-stability concept

Farshid Habibi *, Ali Hesami Naghshbandy, Hassan Bevrani

Department of Electrical and Computer Engineering, University of Kurdistan, Sanandaj, PO Box 416, Kurdistan, Iran

ARTICLE INFO

Article history:
Received 27 April 2012
Received in revised form 3 August 2012
Accepted 9 August 2012
Available online 26 September 2012

Keywords:
Distributed Generation (DG)
Microgrid (MG)
Islanding mode
Robust control
Kharitonov's theorem
D-stability

ABSTRACT

This paper proposes a new robust voltage control strategy for an isolated Microgrid (MG). The MG consists of several Distributed Generation (DG) units and local loads, which should be capable to operate in both connected and disconnected modes. To achieve this goal and suitable performance in both modes, robust control may provide many advantages. The proposed control structure proceeds to design a robust voltage controller based on Kharitonov's theorem for an isolated MG system. It utilizes an internal oscillator to frequency control and a proportional–integral (PI) controller to maintain voltage stability that is tuned by Kharitonov's theorem. For fine-tuning of the PI controller, D-stability concept as a complementary method is used. The PI voltage controller endeavors to minimize errors between direct and quadrature voltage components and their reference values. Performance of the robust voltage control method and isolated MG system are evaluated by several simulations in the presence of uncertainty in the system parameters.

1. Introduction

Nowadays, with increasing energy demand growth and limitations caused by global warming and fossil fuels shortage, the conventional power systems have encountered with many problems. To solve these problems, DG resources introduced as alternative generation units to the modern power systems. They often use renewable energy resources like wind power, solar, geothermal and fuel cells to produce electrical energy. In fact, emerging DGs to the modern power systems are based on three main issues i.e. environmental problems, as well as economic issues, and security supply [2,6,10].

Besides many advantages of the DGs, they make several challenges for power system such as increasing of complexity, changing protection rules, and DGs maintaining [1,2]. To overcome these problems, it is needed that all DGs and local loads be considered integrally and also, new standards for the DGs and bulk grid participation are essential. Hence, Microgrid (MG) concept was introduced into the modern power system. The MG consists of several and small electrical resources such as diesel generators, wind turbines, fuel cells, solar cells, as well as local loads and controllers. The MG concept was formulated in 1998 by the Consortium for Electric Reliability Technology Solutions (CERTSs) that assumes a MG as an aggregation of loads and small sources operating as an independent system to provide both power and heat [12]. DC and AC sources can be utilized in the MGs, therefore majority of the micro sources must be equipped with power electronic interfaces to provide the required flexibility to insure operation as a single aggregated system. This approach allows the MGs to present itself to the main grid as an independent unit which can provide reliable and secure power to its local loads in both connected/disconnected modes [7,13].

The MGs are usually working in connected operating mode, but it is also possible to go in islanded operating mode due to scheduling or in emergency conditions following a severe disturbance occurrence. Hence, the MG systems must be able to provide stable operating in both connected and disconnected modes. To achieve these purpose, several control approaches are introduced which Single Master Operation (SMO) and Multi Master Operation (MMO) are most common ones. In the SMO, a great controllable DG is responsible to maintain system stability, while in the MMO, several DGs are responsible for this issue. The most control methods use droop characteristics of DGs like the active power-frequency (PF), the active power-voltage (PV), the reactive power-voltage (QV), as well as the reactive power-frequency (QF) for adjusting controller parameters and usually, control signals are applied to the power electronic devices like the voltage source converters (VSCs) [14,16].

For fine-tuning of the controllers in the MG systems, different methods such as classical, intelligent and robust methods have been so far reported. However, considering variable nature of the renewable-energy resources, production of these resources would not be easily predictable and always will be associated with

* Corresponding author. Tel.: +98 871 3520820.
E-mail address: farshid.habibi@uok.ac.ir (F. Habibi).

0142-0615/$ - see front matter © 2012 Elsevier Ltd. All rights reserved.
http://dx.doi.org/10.1016/j.ijepes.2012.08.023

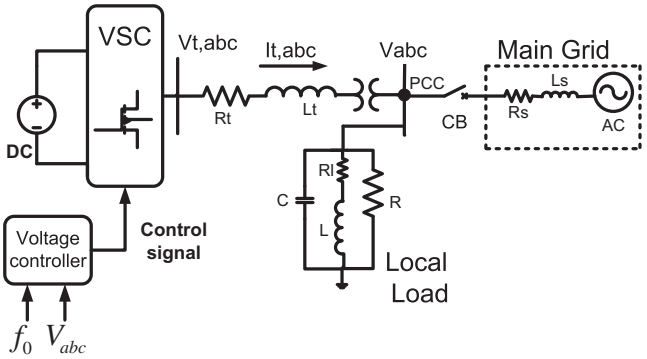

Fig. 1. Simplified schematic diagram of an isolated MG system.

fluctuations. Therefore, the MG systems may be forced to islanded mode, which in this mode due to low inertia, the system stability is often in the critical operation, and the MGs even lead to unstable condition. Hence, robust control is an essential need for stabilizing the isolated MG systems. The main advantage of robust approaches in comparison of other methods is in robustness and adaptiveness against perturbations which exist in the system [17,19].

In the present paper, a robust control method based on Kharitonov's theorem is proposed to design a robust proportional–integral (PI) controller which guarantees satisfactory operation of the MG system under uncertain operating conditions. Then, for fine tuning of the PI controller, D-stability criterion is used. The Kharitonov's theorem addresses few polynomials which obtained from characteristic equation of the closed-loop system. Using the Hurwitz criterion, proper values of proportional and integral gains of the PI controller to stabilize Kharitonov's polynomials, are obtained [3].

This paper is organized as follows: the MG case study, its structure and mathematical model for performance evaluating of the proposed robust voltage control method, in Sections 2 and 3, are described. In Section 4, control design strategy based on Kharitonov's theorem and D-stability concept, will be presented. Simulation results and conclusion are presented in the Sections 5 and 6, respectively.

2. MG case study

Simplified schematic diagram of an isolated MG system is shown in Fig. 1. It contains of a DC voltage source, a DC–AC converter to interface DC voltage source and distribution lines, a filter which represented with R_t and L_t parameters to extract fundamental frequency of terminal voltage, three phase local load represented by a parallel RLC, a three phase transformer in Yn/Δ configuration which transforms voltage from 600 V to 13.8 kV, and a local controller for stabilizing the MG, in both connected/disconnected modes. The main grid is described by R_s and L_s parameters and, an AC voltage source as well. In the Point of Common Coupling (PCC), the MG is connected to the main grid via a circuit breaker (CB). If in the power system, a disturbance such as short circuit or generation unit outage happens, the system may be unable to maintain overall stability in the connected mode, and the MG system may lead to the isolated mode.

The DG unit and local loads (shown in Fig. 1) must be in service in both connected and disconnected modes. In the connected mode, the main grid is responsible to maintain the system voltage and frequency in a permitted bound. In this mode, the VSC controls the active and reactive power exchange with the grid, based on the direct-quadrature current control method. This is known as PQ control method, in which the DG units are controlled to deliver constant active and reactive power to the system. In disconnected mode, the MG system must be able to keep the system frequency and voltage in an acceptable range. This is known as voltage source inverter (VSI) control method, in which the inverter is controlled for voltage and frequency stability preserving in the isolated grid by changing the absorbed active and reactive power from the DG units [9,16,18].

In islanded mode, the VSI can employ an internal oscillator with a constant frequency $\omega_0 = 2\pi f_0$, to generate the modulation signals. As shown in Fig. 1, the nominal frequency and three phase of PCC voltage are used by the voltage control unit.

As mentioned, the voltage controller is adjusted using linear robust method based on Kharitonov's theorem. For this purpose, it is necessary to present a mathematical description for the MG system. The mathematical model and transfer functions of the open-loop and closed-loop systems and their properties are presented in next section.

3. Mathematical model

This section describes mathematical model of the isolated MG (in Fig. 1). The state-space model of the MG system under balanced condition in the abc-frame can be presented as shown in (1), where $V_{t,abc}$, $I_{t,abc}$, V_{abc} and $i_{L,abc}$ are three phase terminal voltages, terminal currents, PCC voltages, and PCC currents of inverter, respectively.

$$\begin{cases} V_{t,abc} = L_t \frac{di_{t,abc}}{dt} + R_t i_{t,abc} + V_{abc} \\ I_{t,abc} = \frac{1}{R} V_{abc} + i_{L,abc} + C \frac{dv_{abc}}{dt} \\ V_{abc} = L \frac{di_{L,abc}}{dt} + R_l i_{L,abc} \end{cases} \tag{1}$$

Using α–β transformation and a rotating reference frame [8,9], the d- and q-axis of the state space variables of the MG system yields the following equations:

$$\begin{cases} \dot{X}(t) = AX(t) + bu(t) \\ y(t) = CX(t) \\ u(t) = v_{td} \end{cases} \tag{2}$$

where

$$A = \begin{pmatrix} -\frac{R_t}{L_t} & \omega_0 & 0 & -\frac{1}{L_t} \\ \omega_0 & -\frac{R_t}{L_t} & -2\omega_0 & \frac{R_t C\omega_0}{L} - \frac{\omega_0}{R} \\ 0 & \omega_0 & -\frac{R_t}{L} & \frac{1}{L} - \omega_0^2 C \\ \frac{1}{C} & 0 & -\frac{1}{C} & -\frac{1}{RC} \end{pmatrix}$$

$$b^T = \begin{pmatrix} \frac{1}{L_t} & 0 & 0 & 0 \end{pmatrix}$$

$$C = \begin{pmatrix} 0 & 0 & 0 & 1 \end{pmatrix}$$

$$X^T = \begin{pmatrix} i_{td} & i_{tq} & i_{Ld} & v_d \end{pmatrix} \tag{3}$$

From Eqs. (2) and (3), transfer function of the v_d/v_{td} can be obtained as given in Eqs. (4) and (5), where v_d and v_{td} are direct voltage components of the PCC and inverter terminal voltages, respectively.

$$\frac{v_d}{v_{td}} = \frac{N(s)}{D(s)} \tag{4}$$

and

$$\begin{cases} N(s) = b_2 s^2 + b_1 s + b_0 \\ D(s) = a_4 s^4 + a_3 s^3 + a_2 s^2 + a_1 s + a_0 \end{cases} \tag{5}$$

The $N(s)$ and $D(s)$ are nominator and denominator of transfer function of the open-loop system, respectively. The a_0, a_1, a_2, a_3, b_0, b_1 and b_2 are nominator and denominator coefficients which can be expressed as follows:

Table 1
Rated values of the system parameters in Fig. 1.

Quantity	Values
R_t	1.5 mΩ
L_t VSC rated power	300 μH
VSC terminal voltage	2.5 MW
PWM carrier	600 V
Frequency	1980 Hz
DC voltage	1500 V
R	76 Ω
L	111.9 mH
C	62.855 μ
Q	1.8
f_0	60 Hz
Transformer voltage ratio	0.6/13.8 kV (Yn/Δ)

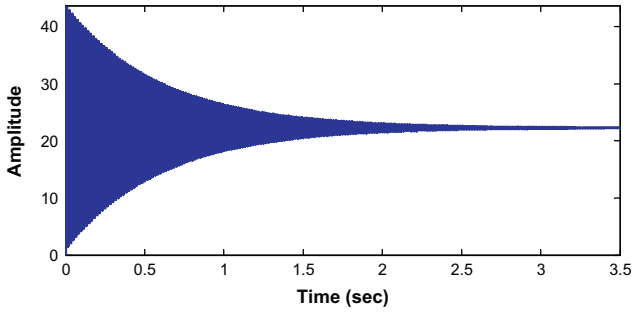

Fig. 2. Step response of the open-loop system.

$$a_4 = L_t R L^2 C$$

$$a_3 = (L_t L^2 + R_t R L^2 C + 2R_t L_t R L C)$$

$$a_2 = (L_t R L + R L^2 + R_t L^2 + 2R_t R_l R L C + 2R_l L_t + R_l^2 L_t R C)$$

$$a_1 = \left(R_t R L + 2R_l R L + R_t R_l^2 R C + R_l L_t R + 2R_t R_l L + R_t \omega_0^2 R L^2 C + R_l^2 L_t + \omega_0^2 L_t L^2 - 2\omega_0^2 L_t R_l R L C\right)$$

$$a_0 = R_t R_l R + \omega_0^2 R L^2 + R_t \omega_0^2 L^2 + R_l^2 R + R_t R_l^2 + \omega_0^2 L_t R L - \omega_0^2 L_t R_l^2 R C - \omega_0^4 L_t R L^2 C$$

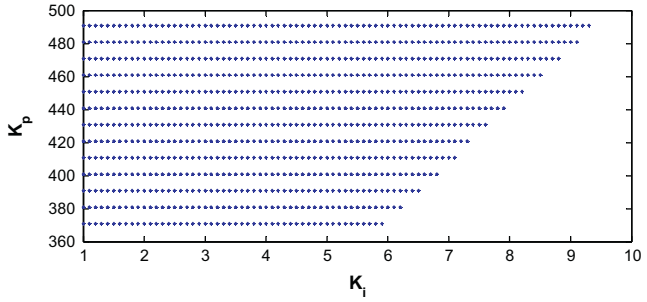

Fig. 4. Stabilizing values of K_p and K_i.

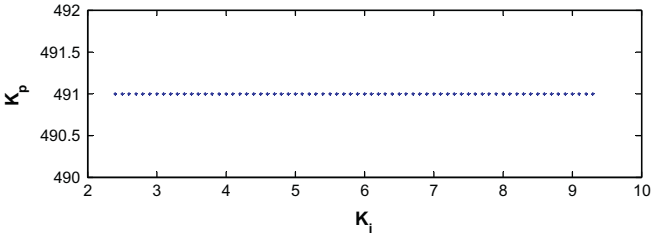

Fig. 5. Separated proper pairs of K_p and K_i using D-stability approach.

$$b_2 = R L^2$$

$$b_1 = R L^2 \left(\frac{2R_l}{L}\right)$$

$$b_0 = R L^2 \left(\frac{\omega_0^2 L^2 + R_l^2}{L^2}\right) \quad (6)$$

As shown in Eq. (5), the MG system has two zeroes and four poles. With substituting rated values of system parameters (Table 1) in Eqs. (5) and (6), transfer function of the plant, $g_n(s)$, is obtained as expressed in (7). The transfer function provides the following features:

- $g_n(s)$ has two zeroes in $-0.0071 \pm 1.78e3i$, hence the plant is a minimum phase system.
- $g_n(s)$ has four poles in $-1.66 \pm 377i$ and $-70.5 \pm 8.82e3i$, therefore the plant is a stable system.

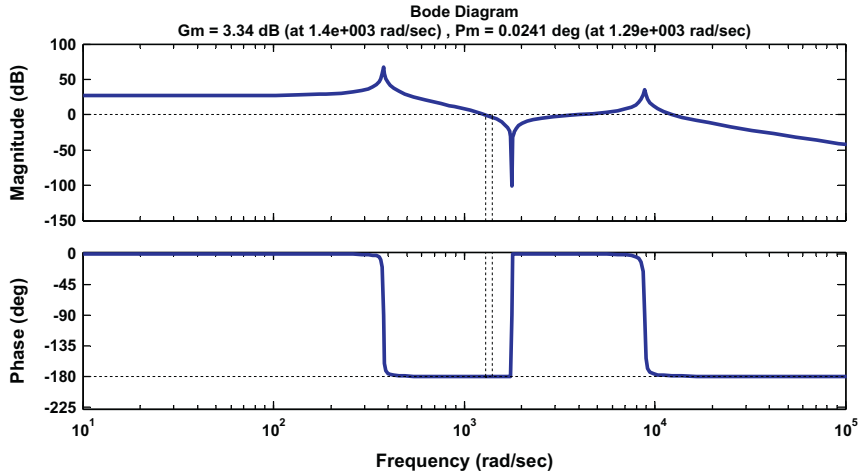

Fig. 3. Open-loop bode diagram of the system.

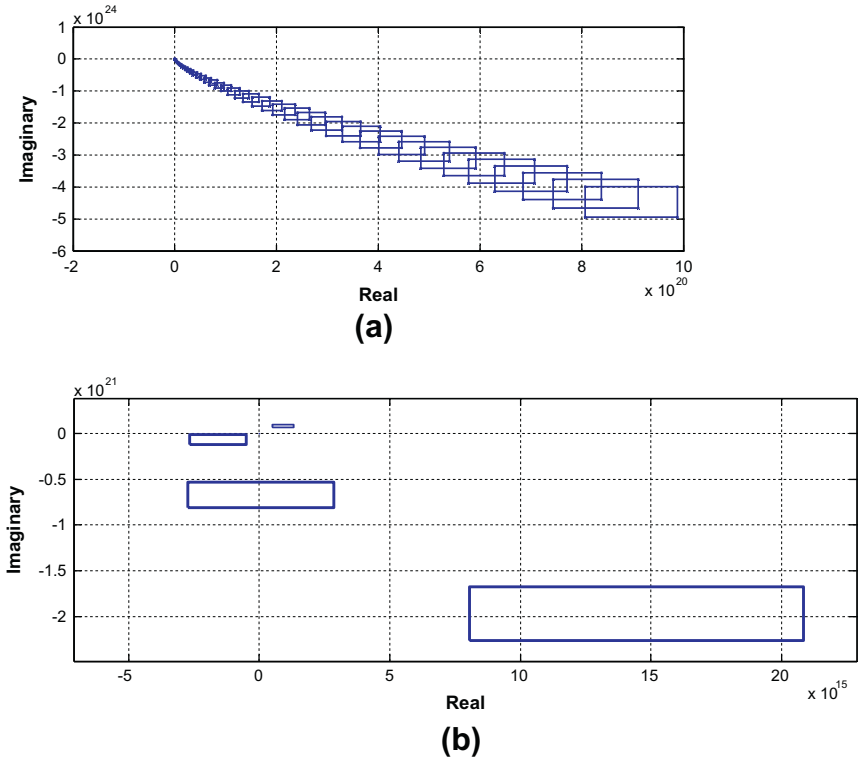

Fig. 6. (a) Motion of the Kharitonov's rectangle for $0 < \omega < 50$ kHz and (b) a magnified view around origin.

Therefore, the MG is a minimum phase and a stable system for the rated values (given in Table 1). But, for other values of *R, L, C* or fluctuation in produced power, change in load pattern and sever faults, the MG may lead to unstable conditions. It is expected that robust control design could be able to guarantee desirable performance in the MG systems in these situations.

$$g_n(s) = \frac{7.778e7s^2 + 1.101e6s + 2.462e14}{s^4 + 144.2s^3 + 7.789e7s^2 + 2.777e8s + 1.105e13} \quad (7)$$

4. Control design strategy

In this section, some essential on the plant and applied control theory are indicated. Then, a robust voltage control design based on Kharitonov's theorem is described for the MG case study. Later, the designed voltage controller is properly tuned by the D-stability criterion. Finally, performance of the proposed control methodology is evaluated by performing several simulations.

4.1. Open-loop system

The open-loop system expressed in Eq. (7). The step response of the open-loop system is shown in Fig. 2. It can be seen that, the MG is an oscillatory system with a significant overshoot in the amplitude. Bode diagrams of the open-loop system is also shown in Fig. 3. The gain and phase margins are 3.34 dB and 0.0241°, respectively which shows low stability margin of the open-loop MG system.

4.2. Kharitonov's theorem

Based on Kharitonov's theorem, every polynomial such as $K(s)$,

$$K(s) = c_0 + c_1 s + c_2 s^2 + c_3 s^3 + c_4 s^4 + \ldots \quad (8)$$

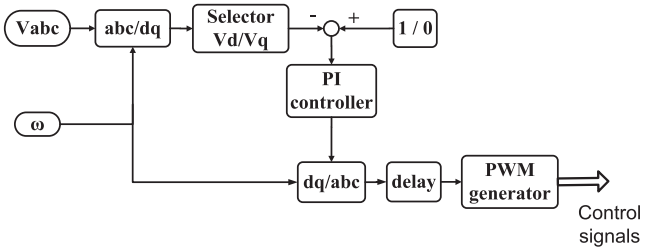

Fig. 7. Applied voltage control structure for the MG case study.

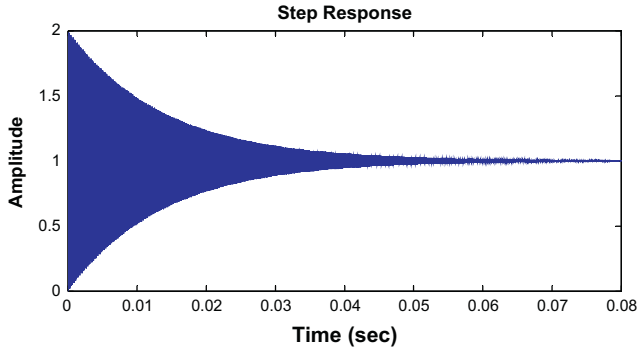

Fig. 8. Step response of the closed-loop system.

with real coefficients is Hurwitz if and only if the following four extreme polynomials are Hurwitz [3].

$$\begin{cases} K_1(s) = c_0^+ + c_1^+ s + c_2^- s^2 + c_3^- s^3 + \ldots \\ K_2(s) = c_0^- + c_1^- s + c_2^+ s^2 + c_3^+ s^3 + \ldots \\ K_3(s) = c_0^- + c_1^+ s + c_2^+ s^2 + c_3^- s^3 + \ldots \\ K_4(s) = c_0^+ + c_1^- s + c_2^- s^2 + c_3^+ s^3 + \ldots \end{cases} \quad (9)$$

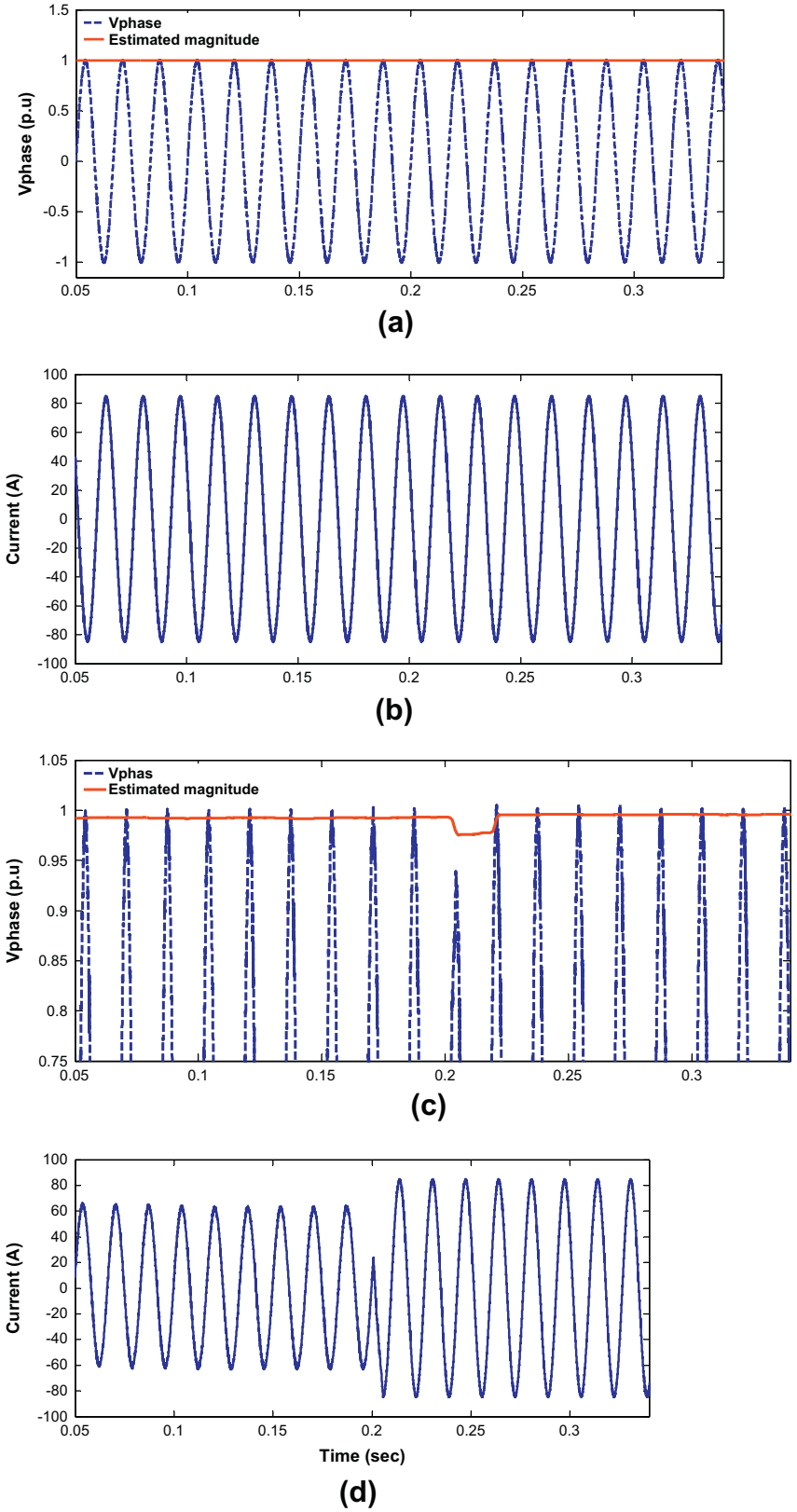

Fig. 9. Pre-fault voltage and current curves for phase-a (a and b), Faulted-on and post-fault curves of voltage, current and real and reactive powers (c–e), *d* and *q* voltage component curves (f), the fault is occurred at 0.2 s.

The "–" and "+" show the minimum and maximum bounds of the polynomial coefficients. In the Kharitonov's theorem, the $K(s)$ is considered as the polynomial characteristic of the closed-loop system.

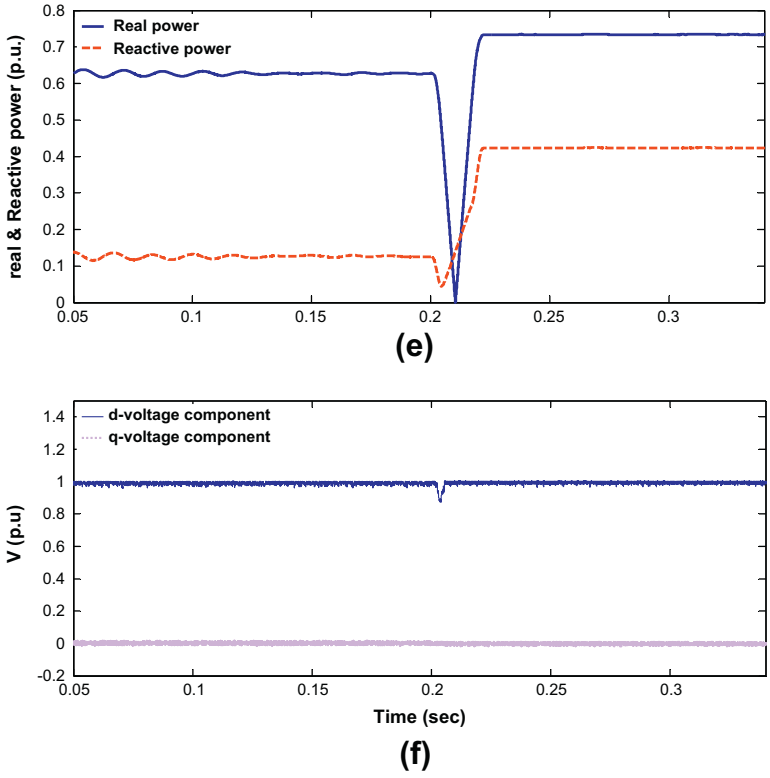

Fig. 9. (*continued*)

Based on a lemma represented in [3,5], for polynomials with orders lower than 5th, there are simpler modes than Eq. (9). For example, for a third-order polynomial, if $C_0^- > 0$, it is just sufficient to check the stability of $K_4(s)$.

For a 4th-order polynomial, the Kharitonov's theorem is reduced to check the stability of $K_1(s)$ and $K_4(s)$, while for a 5th-order it is needed to examine the stability of $K_1(s)$, $K_3(s)$, and $K_4(s)$. Kharitonov's theorem provides a simple and powerful tool for robust adjusting of practical controllers [3].

4.3. Application of Kharitonov's theorem

As described, Kharitonov's theorem is applied to test the stability of polynomial characteristic equation of the closed-loop system. By using a PI feedback controller, the characteristic equation of the closed-loop system can be rewritten as:

$$K_{closed\_loop}(s) = s^5 + c_4 s^4 + c_3 s^3 + c_2 s^2 + c_1 s + c_0 \tag{10}$$

where

$$c_4 = a_3$$

$$c_3 = a_2 + b_2 K_p$$

$$c_2 = a_1 + b_2 K_i + b_1 K_p$$

$$c_1 = a_0 + b_1 K_i + b_0 K_p$$

$$c_0 = b_0 K_i \tag{11}$$

Here, a_i for $i = 1, 2, 3$ and b_j for $j = 1, 2$ are nominator and denominator coefficients of the open-loop system transfer function which described by (6) and, K_p and K_i are proportional and integral gains of the PI controller, respectively. As given in Eq. (10), order of the closed-loop system is 5, and for applying Kharitonov's theorem on a 5th order characteristic equation, it is just needed to test the Hurwitz criterion for the following three polynomials:

$$\begin{cases} K_1(s) = c_0^+ + c_1^+ s + c_2^- s^2 + c_3^- s^3 + c_4^+ s^4 + c_5^+ s^5 \\ K_3(s) = c_0^- + c_1^+ s + c_2^+ s^2 + c_3^- s^3 + c_4^- s^4 + c_5^+ s^5 \\ K_4(s) = c_0^+ + c_1^- s + c_2^- s^2 + c_3^+ s^3 + c_4^+ s^4 + c_5^- s^5 \end{cases} \tag{12}$$

4.4. Robust PI controller design

It is assumed that with ±10% change in the rated values of the system parameters (in Table 1), the open-loop system coefficients (6) being bounded as follows:

$$[a_0^+, a_0^-] = [1.2155e+13, 9.9452e+12]$$

$$[a_1^+, a_1^-] = [3.0545e+08, 2.4991e+08]$$

$$[a_2^+, a_2^-] = [8.5682e+07, 7.0103e+07]$$

$$[a_3^+, a_3^-] = [1.5863e+02, 1.2979e+02]$$

$$[b_0^+, b_0^-] = [2.7081e+14, 2.2157e+14]$$

$$[b_1^+, b_1^-] = [1.2113e+06, 9.9108e+05]$$

$$[b_2^+, b_2^-] = [8.5559e+07, 7.0003e+07] \tag{13}$$

The normalized polynomials characteristic equation of the closed-loop system including a PI feedback controller was described in (10). As indicated, for applying Kharitonov's theorem, it is just needed to check the Hurwitz criterion for three polynomials given in (12). Some algebraic operations result a set of nine inequalities which are presented in the appendix. These inequalities are satisfied for some K_p and K_i as shown in Fig. 4.

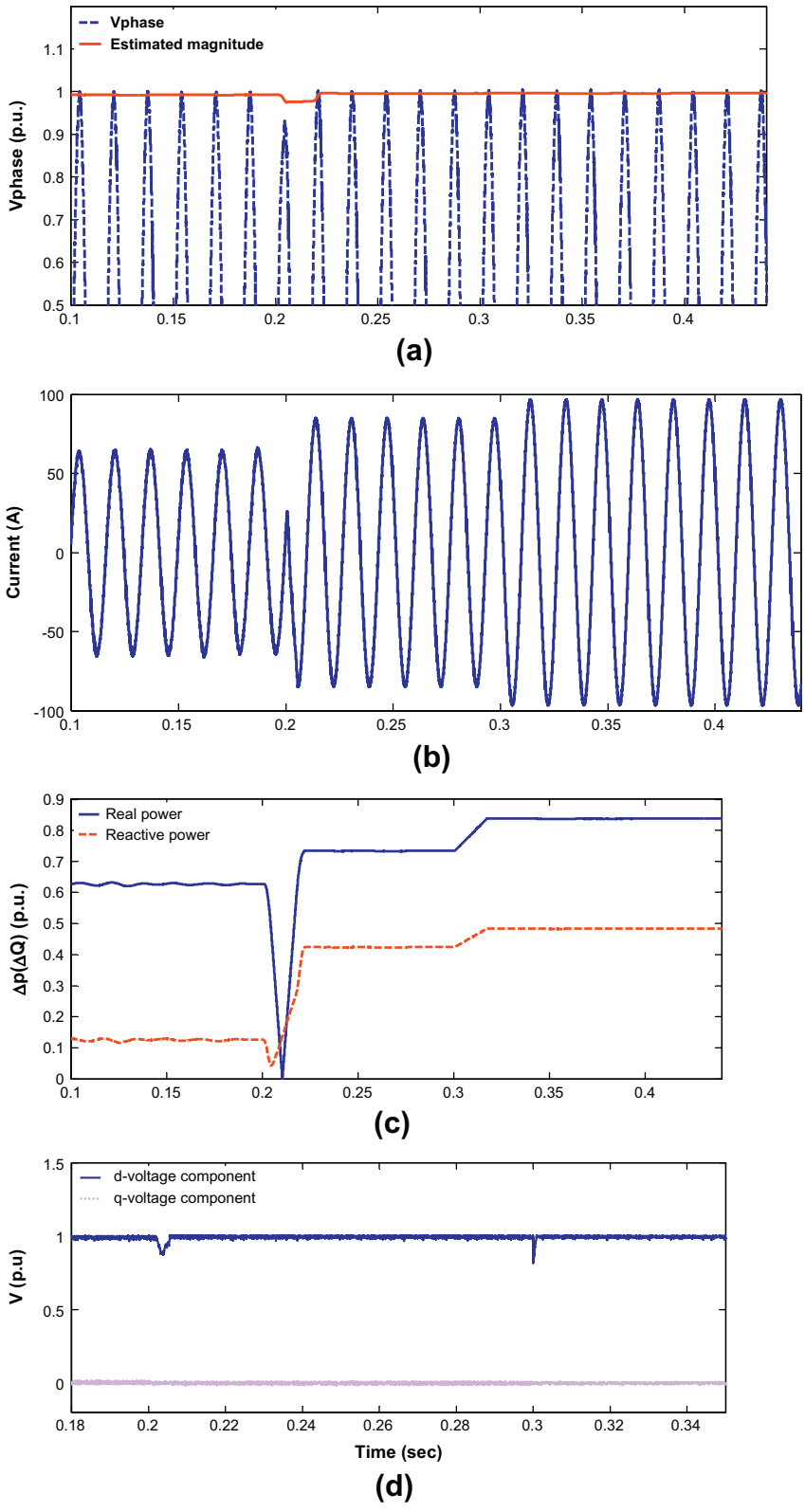

Fig. 10. The PCC voltage after a step load disturbance in real load (a), the PCC current after a step change in real load (b), the active and reactive power curves (c), *d* and *q* voltage component curves (d), the step load disturbance is occurred at 0.3 s.

4.5. Fine tuning using D-stability concept

To ensure both robust stability and robust performance (e.g. desirable transient response) it is important to keep the roots of the polynomial characteristic equation in a specific region (D region). As shown in Fig. 4, there are numerous pairs of K_p and K_i for selection. Using D-stability approach, the most suitable values of K_p and K_i to keep the roots of characteristic equation in specified

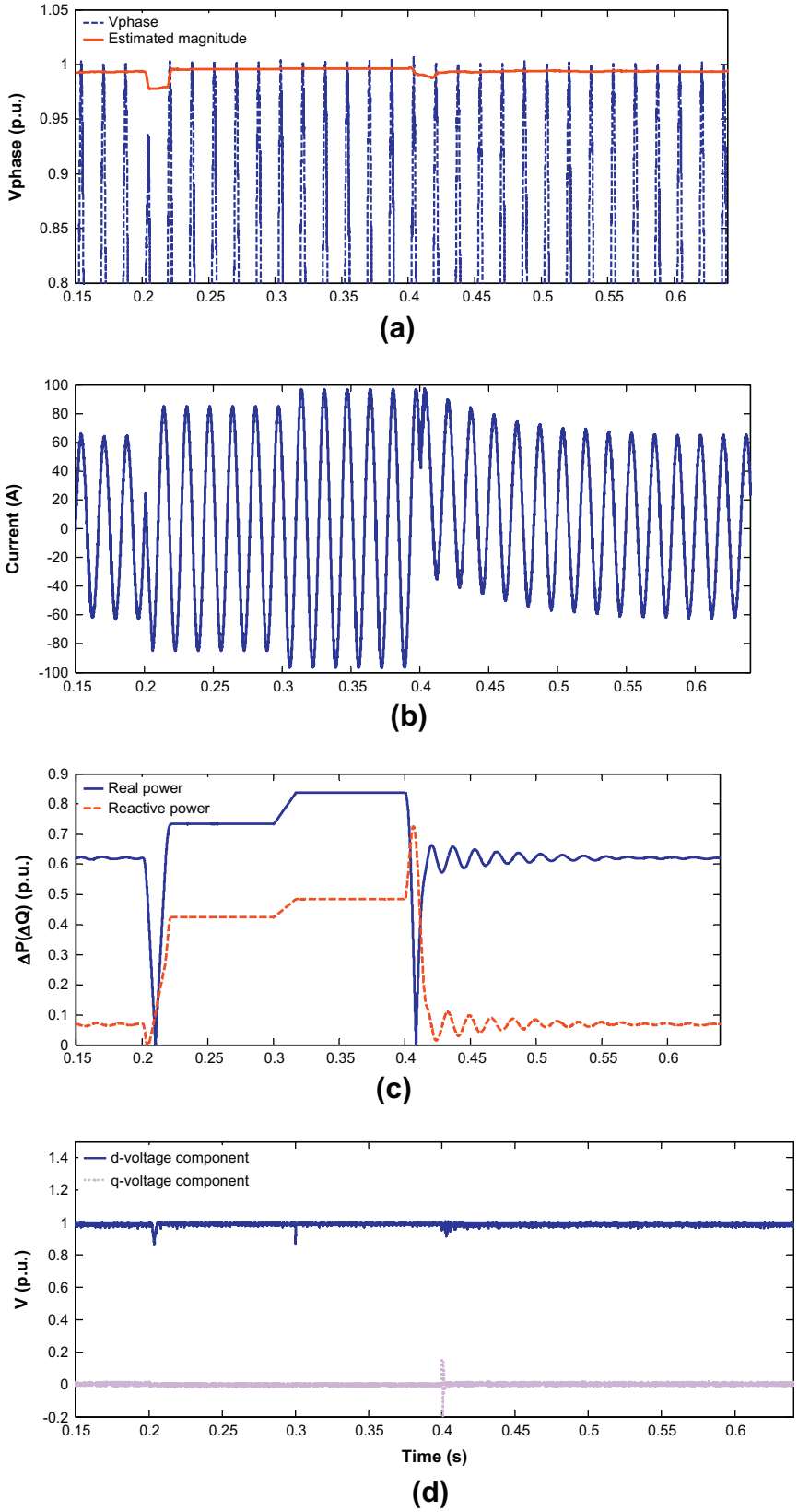

Fig. 11. Reconnection to the main grid at 0.4 s: (a) the PCC voltage and its estimated magnitude, (b) the PCC current, (c) real and reactive power curves, (d) direct and quadrature voltage components.

region, can be selected (Fig. 5). Here, according to Fig. 5, the PI controller parameters are fixed at $K_p = 491$ and $K_i = 9.4$.

The basic geometry associated with the zero exclusion condition [3–5], for $0 < \omega < 50$ kHz, is fully demonstrated in Fig. 6. Based

on the zero exclusion condition closed-loop system with designed PI controller is robustly stable if and only if, the rectangle plots do not include the origin of plane. This issue is clearly confirmed in Fig. 6a and b.

4.6. Voltage control framework

Voltage stability is the ability of a power system to preserve steady state of voltages at all buses in the power system under normal operating conditions and, after occurring different disturbances [11,15]. Proposed control framework for system voltage control is shown in Fig. 7, in which V_{abc} is converted to the dq voltage components. Direct voltage component is compared with 1, and quadrature voltage component is compared with 0. The resulted errors will be minimized with the robust PI controller. The PI controller parameters as described, were fixed at $K_p = 491$ and $K_i = 9.4$. Once again, the dq voltage components are converted to the abc-frame and after a delay block and a PWM generator, the control action signals to control the VSC are provided.

5. Performance evaluation

In this section, some properties of the closed-loop system are presented. Then, the MG system performance is evaluated via several simulations in the MATLAB/SIMULINK environment.

5.1. Closed-loop system features

With substituting values of K_p and K_i which were obtained following the application of Kharitonov's theorem and D-stability approach on the MG polynomial characteristic Eq. (10), the characteristic equation of the closed-loop system is determined as follows:

$$T(s) = s^5 + 144.2s^4 + 3.827e10s^3 + 1.55e9s^2 + 1.209e17s + 2.314e15 \quad (14)$$

Step response of the closed-loop system is shown in Fig. 8. Comparing the results shown in Figs. 2 and 8, it can be realized that overshoot, settling time and transient behavior of the system are significantly improved.

5.2. Dynamic response following islanding

The MG and main grid are commonly supplying a real load at 1.43 MW, while a reactive load at 710 KVAR is supplying by the main grid. For a disturbance occurring in the PCC, the MG is separated from the main grid. After separation, the MG system must be able to keep the local load. This capability is shown in Fig. 9. In Fig. 9a and b voltage and current of one phase at the PCC before disturbance occurring are shown. At 0.2 s, the disturbance is occurred and the CB is opened. Following this event, the MG operation is transferred to the islanded mode. After islanding detection the voltage and current curves at the PCC, are shown in Fig. 9c and d, respectively. From Fig. 9c, it can be seen that the proposed control strategy provides a desirable voltage performance. The voltage profile has been stabilized after a small time about one cycle. As shown in Fig. 9e, after islanding the MG must supply its real and reactive load alone. Statuses of the direct and quadrature voltage components before and after disturbance occurring is also shown in Fig. 9f. These components have been fixed at their reference values. The reference values are considered as 1 and 0 for the direct and quadrature voltage components, respectively.

5.3. System response in the presence of load perturbation

Dynamic Response of the MG system was evaluated following the MG system separation from the bulk grid. The performance of the proposed robust control methodology is examined against a severe step load disturbance of the 300 kW and 100 KVAR at 0.3 s, while the rated power of the system and VSC is fixed at 2.5 MW.

Impacts of the load disturbance are shown in Fig. 10. The voltage and current curves after these perturbations are shown in Fig. 10a and b, respectively. As can be seen following disturbance accruing, the PCC voltage and current signals are properly stabilized and are returned to their ultimate values.

Increasing in real and reactive power in the MG system following load disturbance is shown in Fig. 10c. The direct and quadrature voltage components are also shown in Fig. 10d which are regulated on their reference values as well. Impact of the load disturbance on the voltage profile is clearly specified by Fig. 10d.

5.4. Going back to the connected mode

As shown in the simulations, the MG system could effectively handle disconnecting mode and disturbance load occurring in the islanded mode, suitably. In the following, the MG system performance is evaluated when the MG is going back to the connecting mode. For this sake, after occurring islanding and load disturbance at 0.2 s and 0.3 s, the MG system reconnects to the main grid at 0.4 s and, at same time load disturbance is removed. The MG system response after these changing is plotted in Fig. 11. It can be seen that, the proposed control method can properly handle this scenario, as well.

When the MG reconnects to the main grid, the voltage profile is stabilized after a small variation as shown in Fig. 11a. Returning of the PCC current, real and reactive powers to the nominal values are also shown in the Fig. 11b and c, respectively. Impact of the restoration on direct and quadrature voltage components can be seen in Fig. 11d.

6. Conclusion

A significant feature of a MG is ability to supply its local loads in both connected and disconnected modes. To achieve this goal effectively, in the presence of perturbations and severe faults robust control may needed. In this paper, a robust PI-based voltage controller based on Kharitonov's theorem is designed. For fine tuning of the obtained controller, D-stability concept is used as a complementary synthesis step.

Robustness of the proposed controller is evaluated via several simulations in the MATLAB/SIMULINK environment.

Appendix A. Appendix

The obtained nine inequalities from applying Kharitonov's theorem to make Hurwitz (13) are as follows:

$$\begin{cases} a_2^- < a_3^- a_4^+ \\ -(a_2^-)^2 + a_2^- a_3^- a_4^+ - (a_4^+)^2 a_1^+ > -a_0^+ a_4^+ - (a_4^+)^3 (a_1^+)^2 + 2a_0^+ a_1^+ (a_4^+)^2 + a_0^+ a_2^- a_3^- + a_1^+ a_2^- a_3^- (a_4^+)^2 \\ -a_1^+ a_4^+ (a_2^-)^2 > (a_0^+)^2 a_4^+ + a_0^+ (a_3^- a_4^+)^2 \end{cases}$$

$$\begin{cases} a_2^+ < a_3^- a_4^- \\ -(a_2^+)^2 + a_2^+ a_3^- a_4^- - (a_4^-)^2 a_1^+ > -a_0^- a_4^- - (a_4^-)^3 (a_1^+)^2 + 2a_0^- a_1^+ (a_4^-)^2 + a_0^- a_2^+ a_3^- a_4^- \\ +a_1^+ a_2^+ a_3^- (a_4^-)^2 - a_1^+ a_4^- (a_2^+)^2 > (a_0^-)^2 a_4^- + a_0^- (a_3^- a_4^-)^2 \end{cases}$$

$$\begin{cases} a_2^- < a_3^+ a_4^+ \\ -(a_2^-)^2 + a_2^- a_3^+ a_4^+ - (a_4^+)^2 a_1^- > -a_0^+ a_4^+ - (a_4^+)^3 (a_1^-)^2 + 2a_0^+ a_1^- (a_4^+)^2 + a_0^+ a_2^- a_3^+ a_4^+ \\ +a_1^- a_2^- a_3^+ (a_4^+)^2 - a_1^- a_4^+ (a_2^-)^2 > (a_0^+)^2 a_4^+ + a_0^+ (a_3^+ a_4^+)^2 \end{cases} \quad (15)$$

References

[1] Ackermann T, Andersson G, Soder L. Distributed generation: a definition. Int J Electr Power Syst Res 2001;57:195–204.

[2] Barker P, De Mello R. Determining the impact of distributed generation on power systems. I. Radial distribution systems. In: IEEE power engineering society summer meeting, Seattle, WA, USA; 2001.

[3] Barmish BR. New tools for robustness of linear systems. Macmillian; 1994.

[4] Bevrani H, Abrishamchian M, Safari-Shad N, Nader. Nonlinear and linear robust control of switching power converters. In: Proceedings IEEE international conference on control applications, Hawaii, USA; 1999. p. 808–13.

[5] Bevrani H, Babahajyani P, Habibi F, Hiyama T. Robust control design and implementation for a quadratic buck converter. Int Power Electron Conf 2010;2010:99–103.

[6] Chowdhury C, Chowdhury SP, Crossley P. Microgrids and active distribution networks. London, United Kingdom: The Institution of Engineering and Technology; 2009.

[7] Gabbar HA, Islam R, Isham MU, Trivedi V. Risk-based performance analysis of microgrid topology with distributed energy generation. Int J Electr Power Energy Syst 2012;43:1363–75.

[8] Karimi H, Davison EJ, Iravani R. Multivariable servomechanism controller for autonomous operation of a distributed generation unit: design and performance evaluation. IEEE Trans Power Syst 2010;25(5).

[9] Karimi H, Nikkhajoei H, Iravani R. Control of an electronically-coupled distributed resource unit subsequent to an islanding event. IEEE Trans Power Deliv 2008;23(1).

[10] Khani D, Sadeghi Yazdankhah A, Madadi Kojabadi H. Impacts of distributed generations on power system transient and voltage stability. Int J Electr Power Energy Syst 2012;43:488–500.

[11] Kundur P, Paserba J, Ajjarapu V, Hill, Dagle J, Stankovic A, et al. Definition and classification of power system stability IEEE/CIGRE joint task force on stability terms and definitions. IEEE Trans Power Syst 2004;19(3):1387–401.

[12] Lasseter RH, Akhil A, Marnay C, Stephens J, Dagle J, Guttromson R, et al. The CERTS microgrid concept. In: White paper for transmission reliability program. Office of Power Technologies, U.S. Dept. Energy; April 2002.

[13] Lasseter RH, Eto JH, Schenkman B, Stevens J, Vollkommer H, Klapp D, et al. CERTS microgrid laboratory test bed. IEEE Trans Power Deliv 2011;26(1):325–32.

[14] Lopes JAP, Moreira CL, Madureira AG. Defining control strategies for MicroGrids islanded operation. IEEE Trans Power Syst 2006;21(5):916–24.

[15] Oshiro M, Tanaka K, Senjyu T, Toma S, Yona A, Saber AY, et al. Optimal voltage control in distribution systems using PV generators. Int J Electr Power Energy Syst 2011;33:485–92.

[16] Serban E, Serban H. A control strategy for a distributed power generation MG application with voltage and current-controlled source converter. IEEE Trans Power Electron 2010;25(5).

[17] Sofla MA, Gharehpetian GB. Dynamic performance enhancement of microgrids by advanced sliding mode controller. Int J Electr Power Energy Syst 2011;33:1–7.

[18] Song H, Nam K. Dual current control scheme for PWM converter under the unbalanced input voltage conditions. IEEE Trans Ind Electron 1999;46(10):953–9.

[19] Vachirasricirikul S, Ngamroo I. Robust controller design of microturbine and electrolyzer for frequency stabilization in a microgrid system with plug-in hybrid electric vehicles. Int J Electr Power Energy Syst 2012;43:804–11.